quaternary

MDPI

Article

Socio-Ecological Contingencies with Climate Changes over the Prehistory in the Mediterranean Iberia

Elodie Brisset [1,2,3,*], Jordi Revelles [2,3], Isabel Expósito [2,3], Joan Bernabeu Aubán [4] and Francesc Burjachs [2,3,5]

1 IMBE—Institut Méditerranéen de Biodiversité et d'Ecologie, Aix Marseille Univ, CNRS, IRD, Avignon Université, 13545 Aix-en-Provence, France
2 IPHES—Institut Català de Paleoecologia Humana i Evolució Social, 43007 Tarragona, Spain; jrevelles@iphes.cat (J.R.); iexposito@iphes.cat (I.E.); fburjachs@iphes.cat (F.B.)
3 Àrea de Prehistòria, Universitat Rovira i Virgili, 43007 Tarragona, Spain
4 PREMEDOC Research Group, Department of Prehistory, Archaeology and Ancient History, University of Valencia, 46010 Valencia, Spain; Juan.Bernabeu@uv.es
5 ICREA—Catalan Institution for Research and Advanced Studies, Catalonia, 08010 Barcelona, Spain
* Correspondence: elodie.brisset@imbe.fr

Received: 10 June 2020; Accepted: 2 July 2020; Published: 7 July 2020

Abstract: We conducted palynological, sedimentological, and chronological analyses of a coastal sediment sequence to investigate landscape evolution and agropastoral practices in the Nao Cap region (Spain, Western Mediterranean) since the Holocene. The results allowed for a reconstruction of vegetation, fire, and erosion dynamics in the area, implicating the role of fire in vegetation turnover at 5300 (mesophilous forests replaced by sclerophyllous scrubs) and at 3200 calibrated before present (cal. BP) (more xerophytics). Cereal cultivation was apparent from the beginning of the record, during the Mid-Neolithic period. From 5300 to 3800 cal. BP, long-lasting soil erosion was associated with the presence of cereals, indicating intense land-use during the Chalcolithic and Bronze Age periods. The decline of the agriculture signal and vegetal recolonization is likely explained by land abandonment during the Final Bronze Age. Anthropogenic markers reappeared during the Iberian period when more settlements were present. A contingency of human and environmental agencies was found at 5900, 4200, and 2800 cal. BP, coinciding with abrupt climate events, that have manifested locally in reduced spring discharge, an absence of agropastoral evidence, and a marked decline in settlement densities. This case study, covering five millennia and three climate events, highlights how past climate changes have affected human activities, and also shows that people repeatedly reoccupied the coast once the perturbation was gone. The littoral zone remained attractive for prehistoric communities despite the costs of living in an area exposed to climatic hazards, such as droughts.

Keywords: Holocene; paleoenvironment; archaeology; rapid climate changes; 4.2 kyr BP event

1. Introduction

Coastal ecosystems, as dynamic interfaces between land and sea, have been important places of human evolution, migration routes, resource exploitation, and cultural development [1]. In the Mediterranean, human populations on coastal plains increased with the spread of Neolithic culture from the eastern to the western part of the basin [2]. From the Neolithic diffusion onward, the development of food production economies based on agricultural and stockbreeding practices [3], and the importation of exogenic vegetal and animal species [4,5], deeply modified vegetal landscapes [6]. From this starting point to the multifunctional land-use systems, a complex interplay between socio-economic and political contexts, environmental management, and climate changes was involved. The long-term

perspective, over pre- and proto-historical periods, offers a wide view on socio-ecosystem functioning in the context of climate changes and the associated tensions on resources [7].

The region of the Nao Cap (Central-Eastern Spain) is of particular interest for investigating socio-environmental dynamics as this region was a place for the early development of farming practices as far back as the earliest Neolithic groups colonized the Iberian Peninsula 7600–7550 years ago [8]. If the first Neolithic settlements were characterized by sporadic implantations along the seashore and abutting hills [9–11], a rapid diffusion in the hinterland also occurred, following natural corridors, like rivers (e.g., along the Serpis river [9]). The increase in the population and village density from the Bronze Age onward [9,12] has been associated with the development of specialized architectural units [13] dedicated to cattle (e.g., stone enclosures) and food storage (e.g., silos), with the exploited lands occupying increasingly extended geographical areas. Archeobotanical and archeozoological records carried out in archeological sedimentary deposits, especially from the identification of seeds, provided information delineating the evolution of the farming practices [5,14–17], by identifying changes in cereal (e.g., *Hordeum* sp. and *Triticum* sp.) and legume cultivation, as well as the presence of domestic animals (e.g., *Ovis, Capra*, and *Bos taurus*). In archeological records that allow investigation of the vegetation dynamics as well as the agricultural elements (e.g., Cova de les Cendres [18], Les Jovades and Niuet [19], and Mas d'Is [20]), there is no doubt that cultivation was associated with the exploitation of the arboreal strata, which likely brought the dismantling of the Mid-Holocene meso-thermophilous forests forward.

However, while links between the vegetation dynamic and land use are generally well-defined, local specificities appear [21,22], especially in the interface environments, such as coasts. This is the case of the Nao Cap region, which remains unevenly documented in the paleoecological records (the Casablanca-Almenara wetland in Castellón [23], Valencia lagoon [24], Pego-Oliva lagoon [25], and Xàbia bay southern Nao Cap [26]). Those records noticeably lack stratigraphical continuity and sufficient dating for the characterization of prehistoric human engagements, as has been done, for example, in southern France [27,28], in Sardinia [29], in Corsica [30,31] or in northern Mediterranean Spain [32]. Indeed, due to the rapid sea transgression inland during the Mid- to Late-Holocene, coastal sedimentary records generally present high deposition rates and are dominated by sandy materials [33]. These taphonomic conditions particularly affect the preservation of biological indicators of terrestrial origin, such as pollen, and these remains often occur in quantities too low to be statistically representative [34]. Those conditions made finding of suitable sedimentary archives difficult [35]. However, consecutively to the stabilization of the sea-level 7000 years ago, geomorphic systems shifting to river-dominated have occasionally favored the long-term establishment of palustrine and deltaic areas [36], protected from marine influences.

In this context, and based on the paleoecological (pollen, non-pollen palynomorphs, and charcoal) and sedimentological analyses (lithostratigraphy and magnetic susceptibility) conducted on a new, continuous, coastal palustrine sequence from Central Mediterranean Spain (core P17-9, Pego-Oliva, Valencia region, Spain), this paper aimed:

1. to reconstruct the morphogenetic evolution of the coastal plain of Pego-Oliva linked with the Mid-Holocene stabilization of the sea-level rise;
2. to characterize vegetation successions, fire dynamics, and soil erosion at the interface between the coastal plain and abutting hills over the last 7000 years;
3. to decipher the local impacts of the agropastoral activities from the Post-Cardial Neolithic (5000 cal. BCE) to the end of the Iron Age (2000 cal. BCE); and
4. to investigate the influence of three Rapid Climate Changes (at ~5.9, ~4.2, and ~2.8 kyr BP events), on ancient socio-ecosystem functioning.

2. Study Site

The natural reserve of Pego-Oliva, located in the western Mediterranean (Figure 1A), is one of the numerous coastal marshes located along the Spanish littoral (Figure 1B), between the Albufera of

Valencia to the north and the Nao Cap to the south in the continuity of the Aitana mountain range. The littoral area has been the object of systematic geomorphological [26,33,35,37–40] and geophysical investigations [41]. Even if the chronological controls are unequal depending on the sites, altogether, they permitted researchers to reconstruct the main stages of the Holocene evolution. In the Pego-Oliva area in particular [25,33], from ca. 9500 to 8200 calibrated before present (cal. BP), the vertical sea-level rise was translated into an inland coastal migration and the development of a barrier-lagoon system. Those lagoons disappeared at 8200 cal. BP as a result of the marine transgression. At its maximal inland position, dated at 7330 cal. BP, the shoreline was located 4 km from the modern coastline (Figure 1C). Lower sea-level rise rates favored a return to sand spit construction that closed the basin at 5800 cal. BP [33]. From this date, the coastal lagoon of Pego-Oliva progressively silted up, allowing the formation of the present-day marsh at the sea-level elevation, sheltered from the sea by a 1.5 km wide sand bar.

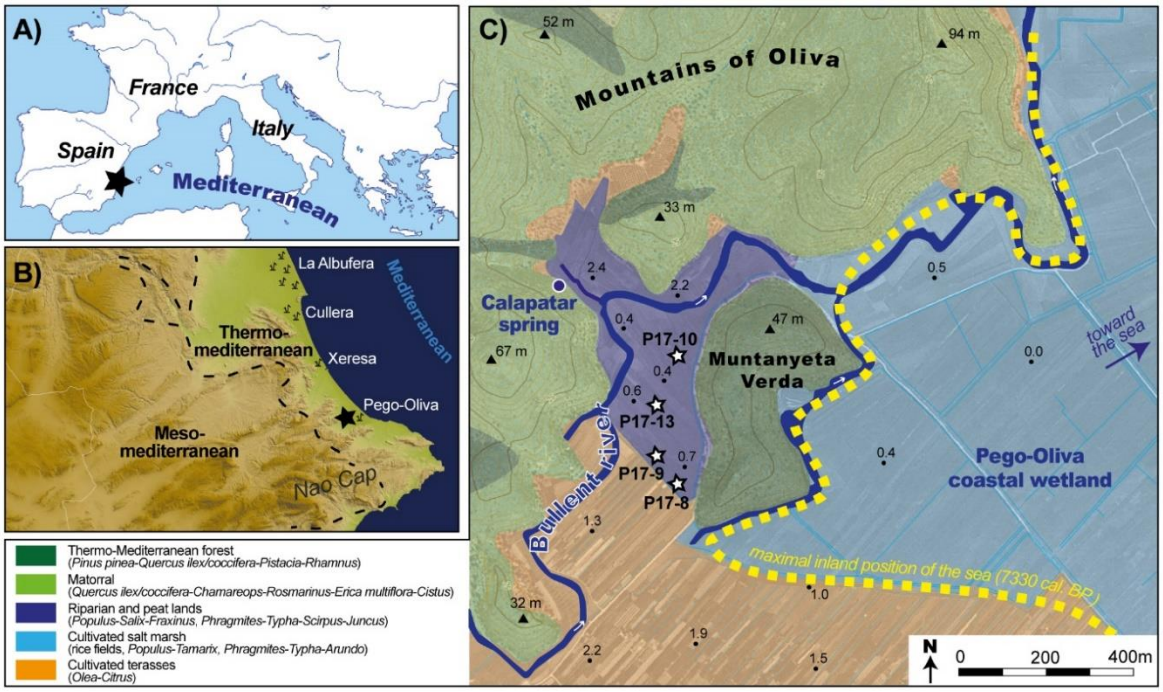

Figure 1. Localization of the study site of Pego-Oliva (**A**) in the Western Mediterranean (black star). (**B**) The coastal band is characterized by the presence of several marshes, including the marsh of Pego-Oliva, located in the Thermo-Mediterranean vegetation belt. The transition between the Thermo- and the Meso-Mediterranean domains is indicated by a dashed line. (**C**) Four sediment cores (P17-8, P17-9, P17-10, and P17-13) were extracted from a peatland (blue) located along the Bullent River, partly separated from the coastal marsh by the small hill of the Muntanyeta Verda, and Pleistocene glacis (orange). The vegetation assemblages are represented using color transparency. The dashed yellow line refers to [33].

The study site is located in the north-western part of the Pego-Oliva marsh bordering the massive dolomite Oliva Mountains (100 m high). This area is characterized by the presence of a peatland of 13 hectares partly separated from the main basin by a small hill (Muntanyeta Verda). This peatland is located along the low-energy meandering Bullent River, which receives a freshwater discharge from lateral aquifer karstic resurgences (e.g., Calapatar spring; Figure 1C) that are particularly rich in calcium carbonates, and which progressively increase in salinity toward the coast [42]. This wetland presents an exceptional location to study coastal vegetation dynamics, connected to the main basin but protected by a small hill, favoring the accumulation of fine-grained organic sediments, great for the preservation of biotic indicators.

The vegetation of the peatland (Figure 1C) is primarily composed of *Typha, Juncus, Phragmites, Scirpus, Potamogeton*, and *Myriophyllum* [43]. Certain riparian trees (*Populus, Salix*, and *Fraxinus*) are present along the Bullent River. The vegetation of this area contrasts with the main basin, which is characterized by rice cultivation associated with a dense network of irrigation channels with an assemblage of *Phragmites-Typha-Arundo* and the presence of salt-tolerant species, noticeably *Tamarix*. Upstream in the valley of Pego, from 1 to 100 m a.s.l., vast glacis are dedicated to the cultivation of *Citrus* and *Olea*. A Thermo-Mediterranean, subhumid assemblage [44,45] was developed on the hillslopes, dominated by a shrub stratum of the evergreen *Quercus coccifera*, the relict palm tree *Chamaerops humilis*, *Erica multiflora*, *Juniperus phoenicea*, *Rosmarinus*, *Lonicera, Rhamnus lycioides*, and *Cistus albidus*. Forested stands of *Pinus pinea*, *Quercus ilex, Olea europaea* var. *sylvestris*, *Pistacia lentiscus*, and *Rhamnus alaternus* are generally restricted to the northern slopes and inner valleys. The climate is typically Mediterranean, characterized by a strong seasonality of the precipitation (median of 126 mm per month in winter and 9 mm in summer) and temperatures (respectively 11 °C and 25 °C).

3. Materials and Methods

Several campaigns of sediment coring have been conducted. First, campaigns of intensive sampling (16 coring sites) were realized over the entire Pego-Oliva basin using mechanical rotary drillers equipped with hydraulic pistons, with the cores stored in plastic core boxes, to characterize the geometry and timing of the sedimentary infill [25,33,42] and to test the potential conservation of paleobotanical contents in various coring locations. Three new sediment cores (P17-9, P17-10, and P17-13) were performed in the peatland of the Bullent River (Figure 1C), using a hand percussion corer and 1 m-long plastic liners to accurately control the sediment depth and compaction due to coring and to avoid contamination.

The sediment cores were opened, described in terms of the color, texture, grain-size, and presence of macroremains, and stored in a cold room (4 °C) at the IPHES laboratory (Tarragona, Spain). To establish the chronology of the deposition, terrestrial vegetal remains (charcoals and peat) were manually picked under binocular and dated by the Radiocarbon Laboratory of Poznan. The radiocarbon ages from this study and the bibliography were calibrated using IntCal13 [46] at a confidence interval of probability of 2σ. The age-depth model (core P17-9) was built using the Clam R package [47], using a smooth spline function, considering the probability density function of the radiocarbon ages. Ten thousand iterations were computed to estimate the best age-depth model and the confidence envelope of probability (2σ).

The magnetic susceptibility of the sediments of cores P17-9 and P17-13 was continuously measured on a Geotek-MSCL core logger equipped with an MS2B Bartington point sensor (Marine Geosciences department, University of Barcelona) at an incremental step of 1 cm in controlled room temperature conditions [48]. The core P17-9 was selected for the further paleobotanical analysis due to the homogeneous organic sediment accumulation over the whole sequence.

The macro-charcoal analysis was conducted on contiguous samples of 30 cm^3 retrieved at 5 cm steps (90 samples), water-sieved at 150 µm [49], and soaked in 33% H_2O_2. The charcoal particles were counted under a binocular loupe at 50× magnification using a reticule grid of 2 × 2 cm square. Three increasing size classes were defined according to the maximal axis length of the particle: 150 µm to 1 mm, 1 to 3 mm, and greater than 3 mm. The charcoal accumulation rate (CHAR, pieces.cm^{-2}·yr^{-1}) was calculated according to the bulk volume and sedimentation rates estimated by the age-depth model.

Volumetric pollen samples (4 and 8 cm^3), obtained every 5 cm on core P17-9, were chemically treated following a standard procedure [50,51] that included digestions in HCl and NaOH, and minerogenic material separation with heavy density Thoulet liquor (2.1 cm^3/g). The samples were diluted in a known amount of glycerin and mounted on slides. The pollen grains were counted using an Olympus B ×43 microscope fitted at ×10 and ×40/60 objectives. Pollen grain identification was carried out using a photograph atlas [52] and the Cerealia-type was defined according to the morphometric criteria [53], i.e., a grain size superior to 40 µm and a pore size greater than 8 µm. Non-pollen palynomorphs followed the classification of [54–56] and were reported according to their

respective percentage among the terrestrial pollen sum. Pollen grains of hygrophyte and aquatic plants (Cyperaceae, *Typha latifolia*, *Typha/Sparganium*, and *Myriophyllum*) and Asteraceae were excluded from the pollen sum to avoid over-representation of the local taxa. A CONISS cluster analysis constrained by depth was applied to identify statistically significant pollen assemblage zones, and drawn using the software Tilia (version 1.7.16, Illinois State Museum, Research and Collection Center. Springfield USA) [57,58].

4. Results

4.1. Sedimentology, Charcoal, and Chronology

A previous drilling campaign in the Pego-Oliva marsh [33] revealed the presence of homogeneous peat sediments along the Bullent River in core P17-8. In this core, at a depth of 550 cm, one radiocarbon age provided an age of 7420–7280 cal. BP (Figure 2). This sequence of homogenous peat was thicker (from 520 cm to the core top) and older than any of the other sites prospected in the Pego-Oliva basin [33]. As it also presents a good preservation of the palynological content, this area was selected to investigate the past vegetation dynamic.

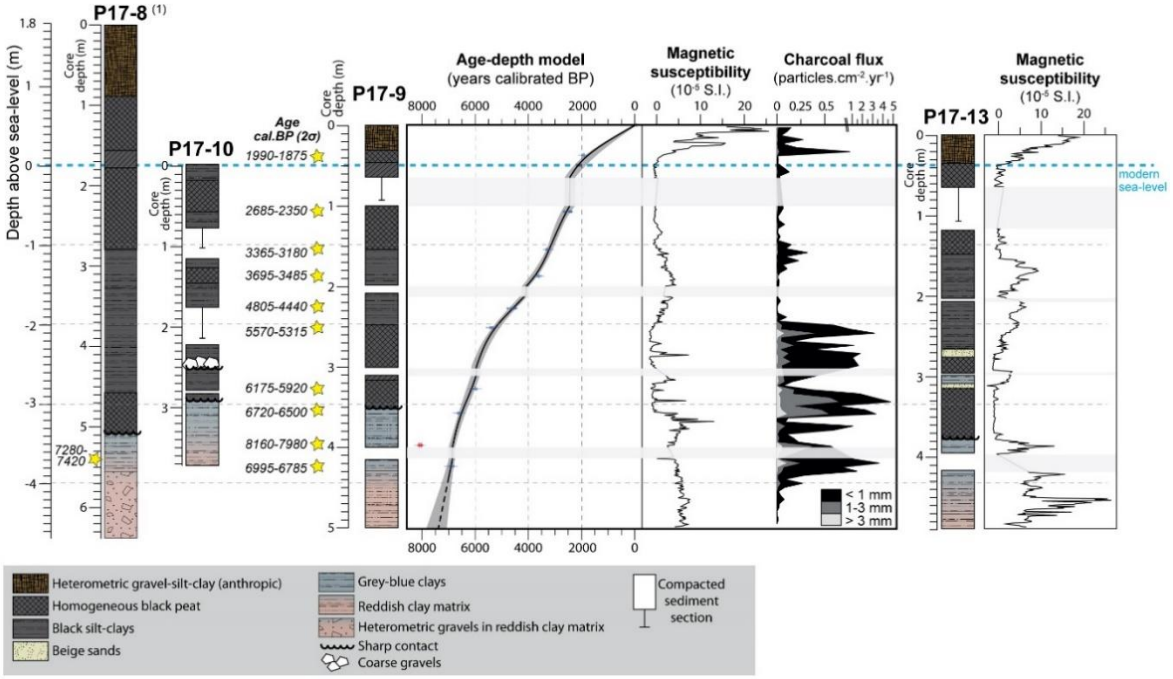

Figure 2. Lithostratigraphy of the sediment cores P17-8, P17-9, P17-10, and P17-13 sampled in the Bullent river peatland. The magnetic susceptibility, charcoal flux, and age-depth model were analyzed on core P17-9. 1 refers to [33].

The cores P17-8 (N 38.87569°; W 0.08774°), P17-9 (N 38.87646°; W 0.08847°), P17-10 (N 38.87847°; W 0.08784°), and P17-13 (N 38.87736°; W 0.08840°) presented similar sedimentary facies successions (Figure 2), with little variations in depth. From bottom to top, the facies succession started with a consolidated unit made of heterometric gravels in a reddish clayey matrix (at 3.8 m b.s.l. (meters below sea-level) in P17-8). The sediment facies progressively changed into reddish and grey-blue detrital clays with high values of magnetic susceptibility (MS) up to a sharp sedimentary hiatus localized between 3 and 3.5 m b.s.l. depending on the cores. From this hiatus a practically uninterrupted accumulation of black organic-rich sediments up to the surface soil started, characterized by lower MS values. This black unit was sub-divided into three facies: homogeneous fibrous peat (3.50–2.45 m in P17-9), a fine gyttja associated with silt-clays (a transitory increase of the MS values) in various proportions depending on the cores (2.45–1.60 m in P17-9), and again, a fibrous peat facies (1.60 m to

30 cm in P17-9). Lateral differences in facies occurred, noticeably from 3.1 to 1.5 m in P17-13; an interval characterized by a higher abundance of silt-clays and the deposition of beige sands. The profiles of magnetic susceptibility measured on P17-9 and P17-13 confirmed those facies similitudes: relative abundances of the minerogenic fraction were similar in both cores; however, P17-13 presented slightly higher values. As the core P17-9 presented similar facies variation compared with the other cores, but presented less compaction due to coring and a more homogeneous organic sequence, this core was selected for further chronological and paleoecological analyses.

The age-depth model of P17-9 was built on nine accepted radiocarbon ages, presenting a good stratigraphical order (Figure 2, Table 1). The age Poz-95364 (397.5 cm) presented an apparent older age regarding the neighbor ages. Considering the dated material and the individual particles of charcoal, this age reversal is likely to be explained by reworking material coming from the surrounding hillslopes. On the whole, the sequence P17-9 covered at least the last 7305–6925 cal. BP (2σ) at 450 cm deep. Core P17-9 consisted of a homogeneous organic sediment accumulation, characterized by a mean sedimentation rate of 0.11 cm·yr^{-1} from 7300 to 5200 cal. BP that decreased to 0.05 cm·yr^{-1} from 5200 to 2000 cal. BP. Pollen samples covered 13 ± 7 yr. The study site is likely to not have recorded more than 7500 cal. BP considering the facies discontinuity to denser, oxidized reddish clays of the bottom core sediments (i.e., 450 to 500 cm) that likely reflect inherited pedogenetic processes from older periods. In the core P17-9, charcoals were essentially recorded as particles of a size smaller than 1 mm (89% of the total); however, in general, the charcoal fluxes of the three sub-size classes presented very similar variations: low from 500 to 450 cm, maximum from 450 to 250 cm, that decreased up to the top core, with a modest re-increase between 190 and 150 cm, and in the upper 40 cm.

Table 1. Radiocarbon ages obtained in the sediment cores P17-8 and P17-9 of the Pego-Oliva wetland and the minimum (min) and maximum (max) 95% confidence interval of calibration (calibration curve: IntCal13) expressed in years calibrated before present (cal. BP). One age, specified in italics, was rejected before the age-depth modeling.

Core Name	Core Depth (cm)	Material	Laboratory Code	Age ^{14}C BP	Min Age cal. BP	Max Age cal. BP
P17-9	37.5	charcoals	Poz-109495	1980 ± 30	1876	1992
P17-9	107.5	charcoals	Poz-109496	2410 ± 30	2351	2684
P17-9	154.5	charcoals	Poz-94011	3065 ± 35	3180	3363
P17-9	187.5	charcoals, peat	Poz-95362	3365 ± 35	3485	3694
P17-9	227.5	charcoals	Poz-109439	4070 ± 35	4438	4804
P17-9	251.5	charcoals	Poz-94012	4675 ± 35	5316	5572
P17-9	327.5	charcoals	Poz-95364	5240 ± 40	5918	6177
P17-9	357.5	charcoals	Poz-95020	5810 ± 40	6498	6718
P17-9	*397.5*	*charcoals*	*Poz-95364*	*7240 ± 40*	*7979*	*8161*
P17-9	423.5	charcoals	Poz-95365	6040 ± 40	6786	6993
P17-8	550.0	charcoals	Beta-460429	6420 ± 30	7280	7421

4.2. Palynology

The mean pollen concentration (3500 pollen grains/gram) and indeterminable taxa (8%) indicate a generally sub-optimal, but sufficient, preservation of the pollen in the homogeneous peat sediments (pollen sum ranging from 200 to 300 grains). As the pollen concentration drops to low values in more minerogenic intervals, 438–390 cm and 221–190 cm (Figure 3A), those intervals are not representative of the vegetation dynamics, and must be interpreted with caution. Two main pollen zones and three sub-zones are defined and described according to the stratigraphically-constrained cluster analysis.

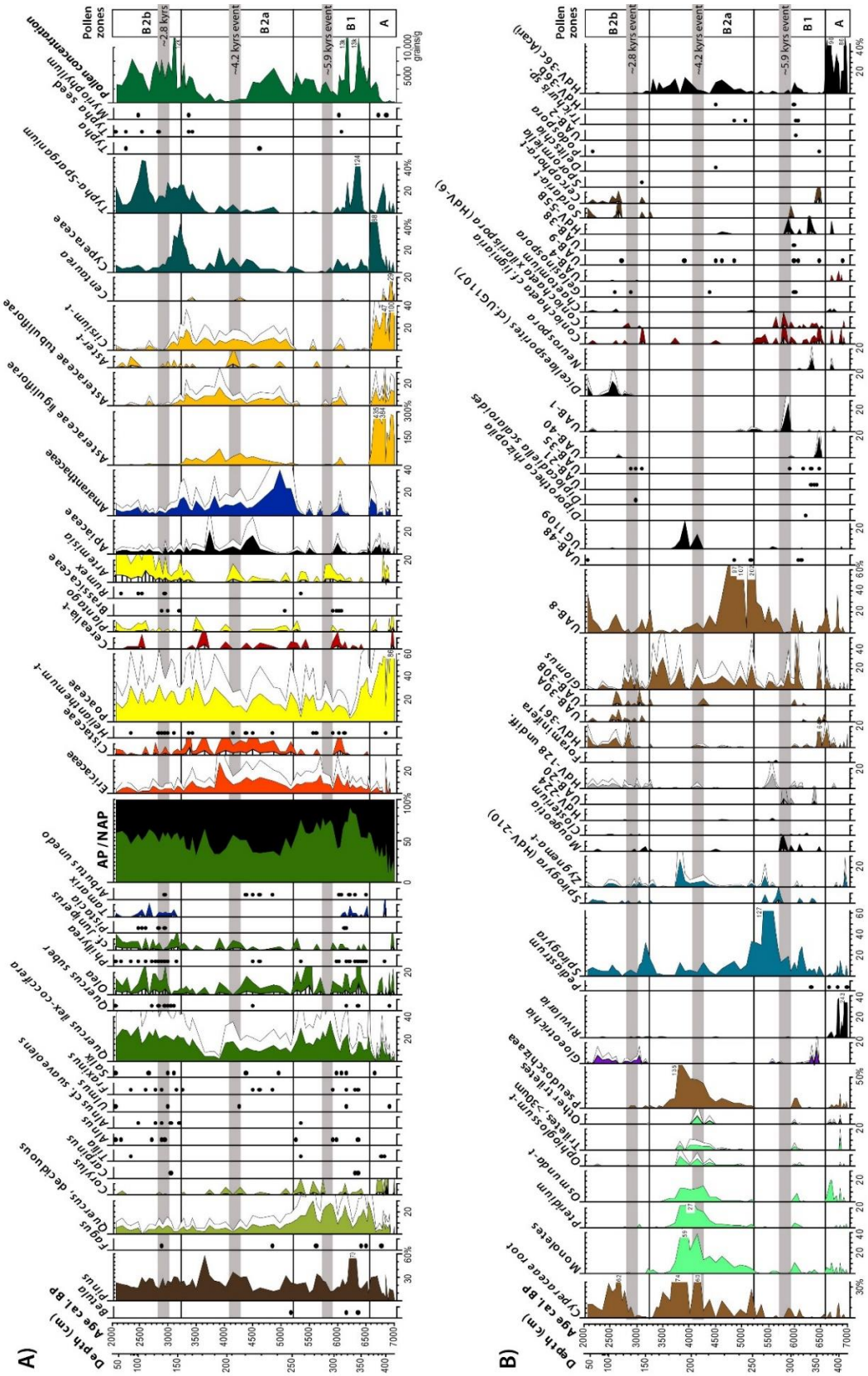

Figure 3. Pollen (**A**) and non-pollen palynomorph (**B**) diagrams of core P17-9, represented in percentages of the terrestrial pollen sum according to the best-modeled ages (calibrated years BP) and the master depth. Hollow exaggeration curves (×2) and color exaggeration curves (×5). Taxa showing low values are represented by dots. AP: arboreal pollen. NAP: non-arboreal pollen.

4.2.1. Zone A (366–438 cm, 7000–6600 cal. BP)

There was a predominance of non-arboreal pollen (NAP). After the exclusion of Asteraceae from the pollen sum, the Poaceae domain in this zone reached 71–86% (Figure 3). This zone is characterized by a high concentration of Asteraceae liguliflorae-t, A. tubuliflorae-t, *Cirsium*-t, and *Centaurea* in certain samples. Among arboreal pollens (AP), *Pinus* showed higher values than *Quercus ilex-coccifera* and deciduous *Quercus*, which are, in this order, the other main taxa. This zone also showed the first evidence of Cerealia-t (434 cm, 7000 cal. BP), and high values of hygrophytes (Cyperaceae and *Typha-Sparganium*) at the end of the zone (366–394 cm), as well as the presence of freshwater algae (*Pediastrum*) and a high concentration of cyanobacteria (*Rivularia*) (Figure 4) and the occurrence of ferns (monolete, *Polypodium, Pteridium*, and *Osmunda*-t), Pseudoschizaea, and carbonicolous-lignicolous fungi (*Coniochaeta* cf. *ligniaria*, *Chaetomium*, UAB-4).

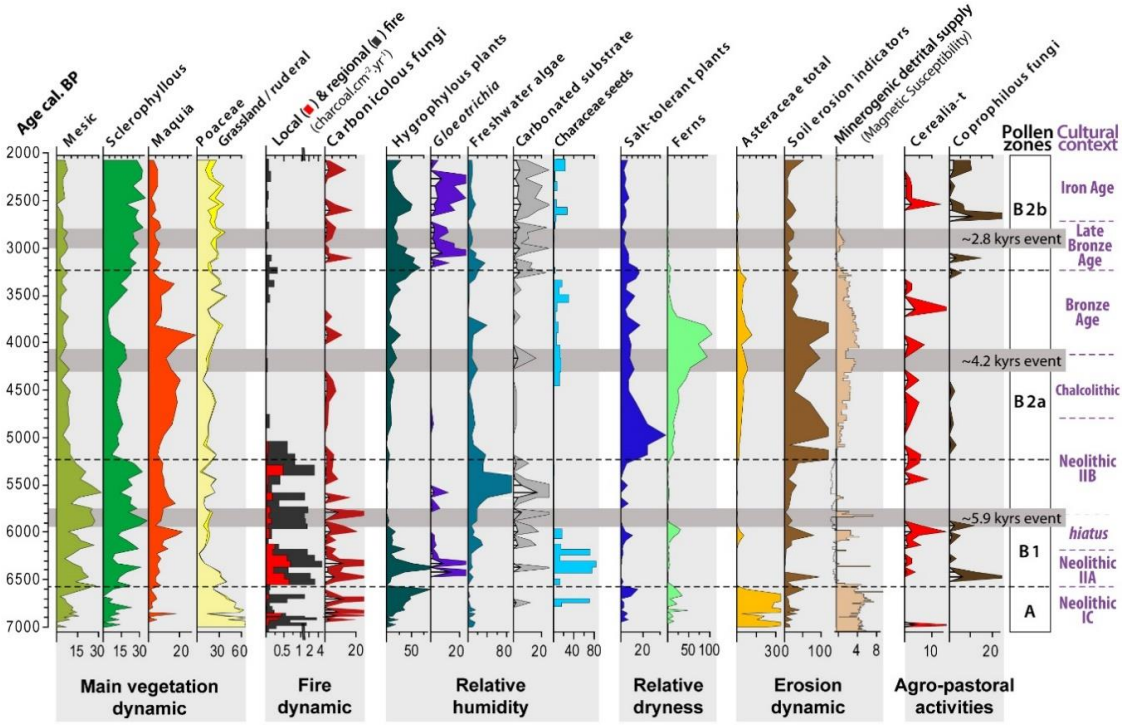

Figure 4. Synthetic pollen and non-pollen palynomorph diagram from core P17-9, together with the Characeae seed abundance, charcoal flux, and magnetic susceptibility. Color exaggeration curves (x5). Categories: mesic (*Quercus* deciduous, *Corylus, Carpinus, Tilia*, and *Fagus*), sclerophyllous (*Quercus ilex-coccifera, Q. suber, Olea, Phillyrea*, and cf. *Juniperus*), maquia (*Pistacia, Arbutus, Erica*, Cistaceae, *Ephedra, Thymelaea*, and *Rhamnus*), grassland and ruderal (Poaceae, *Plantago*, *Artemisia*, Fabaceae, *Galium*-t, Lamiaceae, Brassicaceae, *Polygonum, Urtica*, and *Rumex*), carbonicolous-lignicolous fungi (UAB-4, UAB-9, UAB-12, UAB-38, *Coniochaeta* cf. *ligniaria*, *C. xilariispora* (HdV-6), *Gelasinospora, Chaetomium*, and *Neurospora*), hygrophilous plants (Cyperaceae, *Typha-Sparganium*, and *Typha*), freshwater algae (*Spirogyra, Spirogyra* (HdV-210), *Pediastrum, Zygnema-t, Mougeotia, M. laetevirens-t*, and *Closterium*), aquatic organisms associated with carbonated substrates (HdV-224, UAB-20, and HdV-128 undiff.), salt-tolerant plants (Amaranthaceae and *Typha-Sparganium*), ferns (monolete, *Polypodium*, *Isoetes*, *I. boryana*, *Pteridium, Osmunda*-t, *Ophioglossum*-t, triletes > 50 µm, and other triletes), Asteraceae total (Asteraceae *liguliflorae, A. tubuliflorae*, *Aster*-t, *Cirsium*-t, and *Centaurea*), soil erosion indicators (Pseudoschizaea, *Glomus*, HdV-361, UAB-8, UAB-30A, UAB-30B, UAB-48, and UG-1109), and coprophilous fungi (*Sordaria-t, Cercophora*-t, *Podospora, Delitschia, Sporormiella*, UAB-2, and *Trichuris* sp.).

4.2.2. Sub-Zone B1 (253–362 cm, 6600–5300 cal. BP)

There was an increase in the AP, reaching the highest values in the sequence, related to the increase in both deciduous *Quercus* and *Quercus ilex-coccifera* (Figure 3A), a slight increase in *Erica*, a general decrease in Poaceae, and the occurrence of Cerealia-t, with a peak and continuous curve at 297–394 cm (6800–5900 cal. BP). There is a sharp decrease in Asteraceae. In the first part of this zone (330–350 cm, 6400–6200 cal. BP), hygrophilous plants (Cyperaceae and *Typha-Sparganium*) presented high values. The expansion of ferns with a maximum peak of *Polypodium, Pteridium, Osmunda*-t, *Ophioglossum*-t, and other trilete spores, and also a peak of Pseudoschizaea and *Glomus* were found at 314–330 cm (6200–6000 cal. BP) (Figure 3B). Freshwater algae presented high values, with a maximum concentration of *Spirogyra, Spirogyra* (HdV-210), and *Zygnema*-t, and the occurrence of *Mougeotia*, *Closterium*, and HdV-128 undiff, as well as a peak of *Gloeotrichia* at 6400 cal. BP. We observed the occurrence of a variety of fungal spores (*Diporotheca rhizopila*, UAB-1, UAB-30A, UAB-30B, UAB-21, UAB-35, and *Xylomices* sp. (UAB-40), almost continuous curves of carbonicolous-lignicolous fungi (*Coniochaeta* cf. *ligniaria*, *C. xilariispora* (HdV-6)), and the occurrence of *Neurospora, Chaetomium, Gelasinospora*, UAB-9, and HdV-55B. We also found irregular occurrences of various coprophilous fungi (*Sordaria*-t, *Cercophora*-t, *Podospora*-t, and UAB-2) and parasites (*Trichuris* sp.).

4.2.3. Sub-Zone B2a (154–249 cm, 5200–3200 cal. BP)

This zone is characterized by the sharp decrease in the deciduous *Quercus* values; the regression of *Quercus ilex-coccifera* and AP, in general; the increase in *Erica* and Cistaceae; and the discontinuous occurrence of *Arbutus*, *Olea*, and *Phillyrea*. The expansion of Amaranthaceae was associated with a new phase of high values of Asteraceae and *Cirstum*-t, although a trend of hygrophilous plants expansion culminated at the end of the zone. The occurrence of Cerealia-t and *Plantago* were attested along the entire sub-zone. A high concentration of ferns (monoletes, *Polypodium, Pteridium, Osmunda*-t, *Ophioglossum*-t, and other triletes) and Pseudoschizaea, showed maximum values at 225–241 cm (5000–4500 cal. BP). The regression of freshwater algae and peak of *Glomus*, UAB-8, and UAB-48 at 225–241 cm, low values of carbonicolous-lignicolous, the absence of coprophilous fungi, and the occurrence of *Trichuris* sp. at 237 and 245 cm (4900 and 5100 cal. BP) were noted.

4.2.4. Sub-Zone B2b (48–150 cm, 3200–2000 cal. BP)

This zone is characterized by the recovery of AP, mainly of *Quercus ilex-coccifera*, regression of *Erica*, expansion of *Artemisia*, decrease in Amaranthaceae, and low values of Asteraceae. We noted a peak of Cyperaceae at the beginning of the sub-zone and high values of *Typha-Sparganium* over the entire zone. The occurrence of Cerealia-t at 56–106 cm (2500–2300 cal. BP) was found. The regression of ferns and Pseudoschizaea, high values of cyanobacteria (*Gloeotrichia, Rivularia*), and the continuous curves and high values of freshwater algae and aquatic organisms (*Spirogyra*-t, *Spirogyra* (HdV-210), *Zygnema*-t, *Closterium*, and HdV-128 undiff.) were determined. We observed the regular occurrence of several fungal types (*Glomus*, UAB-8, HdV-361, *Diplocladiella scalaroides*, UAB-30A, 30B, 35, and Dicellaesporites cf. UG1107 [59]), and the occurrence of carbonicolous-lignicolous fungi (*Coniochaeta* cf. *ligniaria*, *C. xilariispora* (HdV-6), *Chaetomium, Gelasinospora*, UAB-4, and UAB-9) and coprophilous fungi (*Sordaria*-t, *Cercophora*-t, *Sporormiella*, and *Podospora*-t).

5. Interpretations and Discussion

5.1. Paludification of River Mouth with the Slowdown of the Sea-Level Rise (7420–6600 cal. BP)

At the contact between the coastal saltmarsh of Pego-Oliva and inherited Pleistocene glacis [60], a sedimentary infilling was deposited associated with the downstream Bullent river mouth, a short- (4 km-long) littoral river fed by freshwater resurgences and superficial runoff. Non-indurated sediments represented a thickness of approximately 5 m, corresponding to an absolute elevation of 4.5 m below sea level (m b.s.l). The soft sediment sequence started with a reddish clay unit that progressively turned

to grey-blue minerogenic sediments (high SM values, Figure 2), dated at 3.8 m b.s.l. of 7420–7280 cal. BP (2σ confidence interval of calibration) in core P17-8. In P17-9, the maximal age was relatively concordant, if even earlier (6990–6785 cal. BP, 2σ), considering a typical spatial variability of riverside sediment infillings, particularly in the initial stages of deposition. The initiation of the deposition was contemporary with the maximal inland transgression of the sea [61]; the river stream base-level being, at this moment, forced by the sea-level position, 3.8 m below the current position [33].

The pollen assemblage was dominated by Asteraceae and Poaceae (Pollen zone A, Figure 3A) associated minor occurrences of a mixture of meso-Mediterranean arboreal taxa (*Pinus*, deciduous *Quercus*, and *Corylus*). We interpret the overrepresentation of Asteraceae and Poaceae as the result of the superficial erosion of Pleistocene sediments (Figure 4). Indeed, the detrital fraction is minerogenic. The occurrence of carbonicolous-lignicolous fungi (i.e., growth on burnt plant remains), of millimeter-size charcoals deposited both in situ as well as reworked (one charcoal sample dated at 8160–7980 cal. BP, 2σ), and of the maximal abundance of Acari microremains likely testify to the erosion of inherited Pleistocene soils (Figure 3B). A similar mixed pollen signal was also found in the littoral sequence of Casablanca-Almenara (Castelló de la Plana) in association with blue-clay sediments at the bottom of the sedimentary sequence, from 4.3 to 3.5 m deep [23], and also in Mazarrón [62]. The high values of hygrophilous plants (i.e., Cyperaceae and *Typha*) with algae as *Rivularia* (pioneer blue-green algae found in nutrient-poor upper littoral saltmarsh) show that the wetland was in an early stage of vegetal colonization, likely influenced by marine water intrusions. Thus, this period mainly reflects a paludification of the littoral linked to a sea-level highstand. The first occurrence of Cerealia-t (Figure 4), a low-dispersion pollen—undoubtedly cultivated [63,64], indicated agricultural practices at least as far as 7000 years ago. The proximity to the Nao Cap mountains, where dozens of Early Neolithic sites have been found [65], and especially to the littoral site of El Barranquet (7550–7310 cal. BP at 2σ [66]), explains the development of cereal culture in the littoral at least as far as the beginning of the P17-9 sequence.

5.2. Optimum of the Mid-Holocene Forest at the End of the Neolithic (6600–5300 cal. BP)

Consecutive to progressive coastal barrier construction from 7300 to 5800 cal. BP [33], the Bullent wetland became shielded from marine erosive agents; meanwhile, the absence of runoff (MS values around zero) created excellent taphonomic conditions for palynology. The pollen assemblage is typical of the Mid-Holocene Climatic Optimum for the south-western Mediterranean [21], as shown by the highest values of deciduous *Quercus* (Figure 3A) and broad-leaf mesic vegetation (Pollen zone B1, Figure 4). The mixed deciduous oak forest was paired with a strong sclerophyllous component, mainly consisting of evergreen *Quercus*, in association with xerophilous maquia scrubs (e.g., Ericaceae, and Cistaceae) and pines. This assemblage was representative of the existing coastal pollen records of southern Spain showing that Mid-Holocene littoral landscapes were dominated by open sclerophyllous forests [21,62,67,68], while thermo-mesophilic forests were situated more inland, at higher altitudes (e.g., Navarrés pollen record, at 225 m a.s.l. in the region of Valencia [69]).

More detailed evidence of the littoral vegetation composition is shown by the anthracological record of the Cova de les Cendres (stratigraphic levels Neolithic II-A and II-B, a cave archeological site located very far eastward in the Nao Cap) that was dominated by *Pinus halepensis* and *Olea europaea sylvestris*, together with *Quercus ilex-coccifera*, *Arbutus unedo*, and *Erica multiflora*. Whereas deciduous *Quercus*, recorded by a continuous presence from the Magdalenian to the Early Neolithic (i.e., over the Lateglacial to about 6000 cal. BP), was no longer present in the record [18]. A similar shift in the deciduous to evergreen oak dominance was observed between the Early and Mid-Neolithic in the anthracological record of the open-air archeological site of Mas d'Is, at 610 m a.s.l. in the center-east of the Nao Cap [70].

In addition to the long-distance dissemination pollen grains typical of the meso-Mediterranean forests (representative of a regional scale), at the local scale, the flora showed more variability of the coastal landscapes. From 6600 to 5900 cal. BP, the occurrence of Cerealia-t and a cortege of coprophilous

fungi provided clear evidence of agropastoral activities taking place along the coast (Figure 4). This result echoes the one found in the coastal pollen record of Casablanca-Almenara (Castelló), where pseudo-continuous occurrences of cereals were found, approximately dated between 6300 and 5300 cal. BP [23]. Agricultural practices were associated with local land management by fire at that period, as this corresponded to near-continuous high values in carbonicolous fungi in the Pego pollen record [55,71], as well as the greatest abundance in macro-charcoals (specifically, the coarsest ones >1 mm). Such practices in the vicinity of the coring site likely had a significant impact on the ecosystem.

High values of hygrophilous plants (Figure 4) and *Gloeotrichia* (cyanobacteria) associated with *Mougeotia* (Figure 3B) reflect a configuration of a vegetated river shore in this newly established peatland before 5900 cal. BP, with probable water eutrophication. This ecological succession could have been a result of the expansion of the riparian trees (*Fraxinus, Salix* in Figure 3A) but could be due to intense anthropogenic disturbances as well. Those results are supported by archeological findings made at the site of El Barranquet, which contained Post-Cardial Early Neolithic ceramics [72]. This site is one of the very few located on the coastline at this period, most of them being rock-shelters located uphill. Indeed, the density of the Neolithic settlements [37,73] in the catchment of Pego (e.g., Cova del Bolumini [74], Figure 5), in the adjacent Serpis valley, as well as at a more regional scale (Figure 6), suggests that human groups were profiting from the large range of biological resources available in this region, for agriculture and animal husbandry as well as fishing in the low-depth brackish waters of the protected lagoon of Pego-Oliva [33].

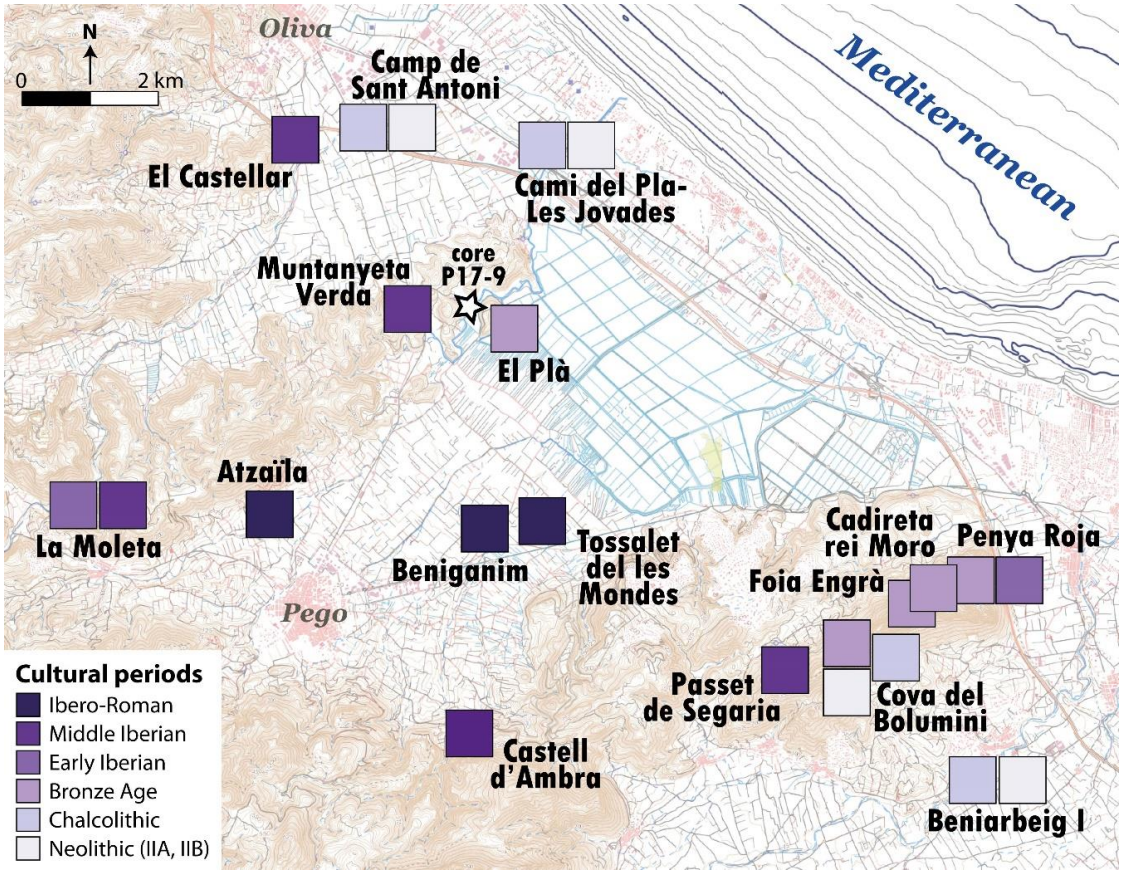

Figure 5. Localization map (topography: brown lines; irrigation channels: light blue lines; bathymetry: dark blue lines) of the archeological sites found in the surroundings of the core P17-9 (star) of Pego-Oliva, and their cultural attribution (simplified), represented by a color gradient. The sites encompassing several cultural layers are represented by adjoining squares (Camp de Sant Antoni, Cami del Pla-Les Jovades, La Moleta, Penya Roja, Cova del Bolumini, and Beniarbeig I). Information was collected from various syntheses [37,75–78].

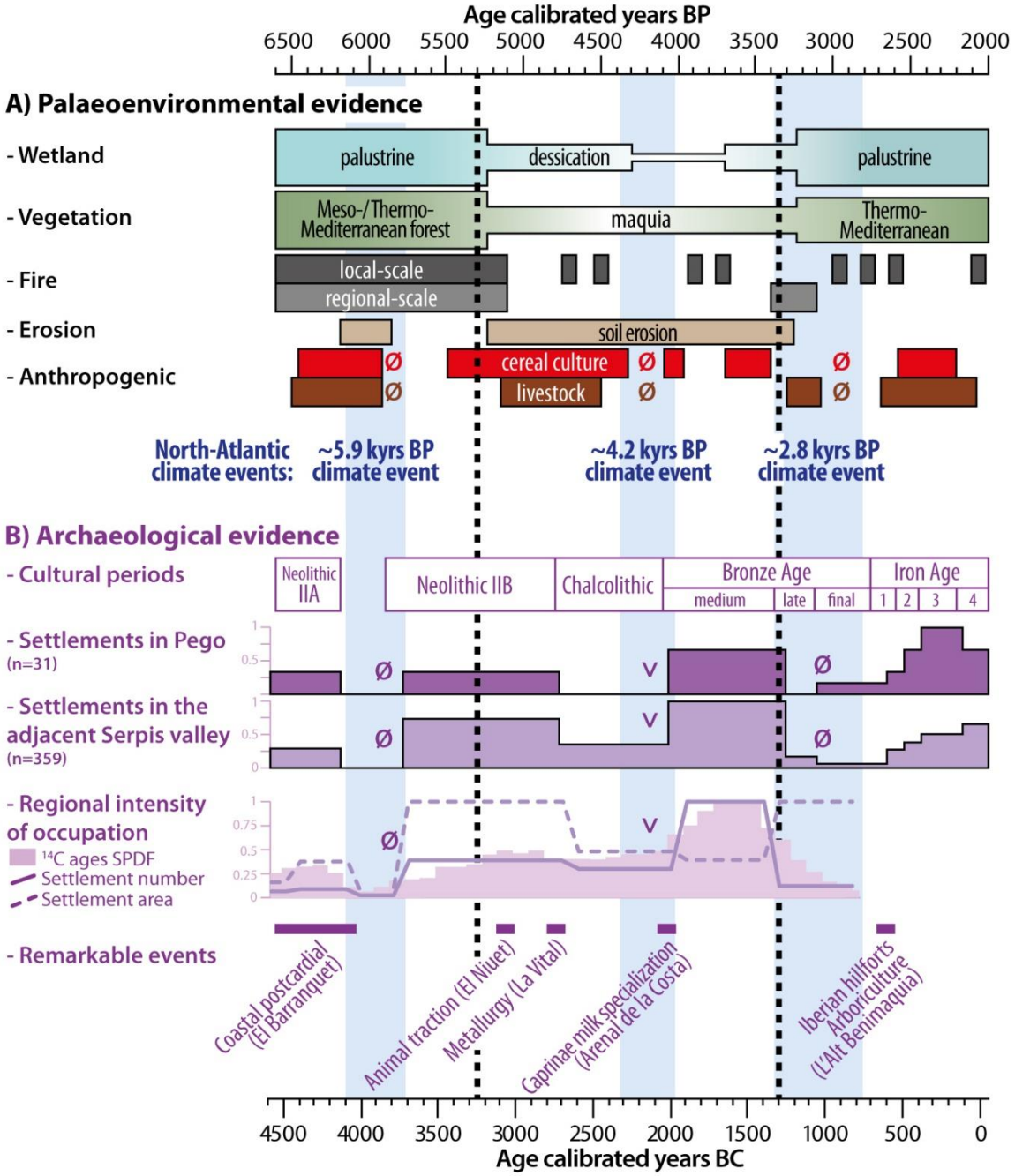

Figure 6. Comparison of the (**A**) paleoenvironmental reconstructions derived from the core P17-9 (Pego-Oliva, this study) represented by varying pipe thicknesses according to the process intensity with (**B**) archeological evidence of occupation in the close (i.e., Pego and Serpis valleys) and large regions (including Pego, Serpis, Albaida, and Canyoles valleys). The proxies of occupation intensity are normalized to 1 (settlement number, settlement areas, ^{14}C ages sum of probability density functions (SPDF)) and represented up to the Bronze Age for the large region [9], and collected from various sources for the first millennium BC [75–78]. The occupation dynamics in Pego were based on only 31 cultural layers (sites are shown in Figure 5), preventing generalization. Reference to the Iberian Iron Age chronology: (1) Orientalism, (2) early; (3) middle, and (4) Ibero-Roman. Selected remarkable innovations are also reported, with mention to the reference sites given in brackets. Ø: absence of evidence; ∨: a marked decrease, discussed in the text. The blue bands highlight periods of increasing ice-rafting debris in the Northern Atlantic [79], typically associated with more aridity in the Iberian Peninsula. The dashed black lines refer to the pollen assemblage zones.

This strong anthropogenic signal temporary disappeared from 5900 to 5500 cal. BP (absence of Cerealia-t and coprophilous spores with low microcharcoal abundance), before recurring at a lower degree at the end of this period, 5300 years ago. In this interval, the wetland was primarily influenced by freshwater habitats (the maximal abundance in freshwater algae, Figures 3B and 4), with high water transparency (e.g., a continuous presence of Characeae and peaks of aquatic organisms related to carbonated substrates). This ecological condition suggested a positive hydrological balance favoring a constant water renewal, likely generated by more active karstic resurgences (Figure 6).

This bi-partition of the record, marked by an interruption of the evidence of agropastoral activities at 5900 cal. BP might be related to a rapid climate change (~5.9 kyr BP event [79], Figure 6), supposedly characterized in south-eastern Iberia by more aridity. Fires, although still well-recorded, are notably characteristic of a long-distance transport (dominance of the particles <1 mm), that supports the hypothesis of a local abandonment of land management practices by fire. A closer look at the pollen diagram may also support this interpretation, with peaks in the Asteraceae, ferns, and soil-erosion indicators (Figure 4) as well as a peak in the minerogenic particles (high MS values). The age-depth model of the core P17-9 dated this detrital crisis at 6285–5870 cal. BP (2σ). A colluvial nappe was also identified in core P17-4 [33] at 5890–5620 cal. BP, consistent with the same morphogenetic event.

Evidence from boreholes are topographically correlated to the coalescent dejection fans occupying the lower part of the catchment—fertile lands intensively exploited for arboriculture today. This interpretation is independently supported by the absence of evidence of Neolithic sites in those geomorphic features, first occupied during the Early Bronze Age (site of El Plà in Figure 5 [80]). If direct regional-scale climatic interpretations would be too prospective based on this very dynamic sedimentation context, we can, however, emphasize the chronological match of the palynological, geomorphological, and archeological records. A major hiatus of occupation occurred at the end of the Neolithic IIA (Figures 4 and 6), dated between 6200–5900 cal. BP [9]. However, if the correlation between phenomena is apparent in the Pego-Oliva region, this is not the case for other regions of the Mediterranean Iberia as has been recently stressed [81]. It might be understood as a particular effect of the climate aridification on the hydrological balance that has been locally superimposed on land-use techniques particularly demanding for soils (e.g., slash-and-burn agriculture), generating soil erosion and sediment alluviation in the lowlands. This convergence of climatic- and anthropogenic-driven environmental changes 5900 years ago may have motivated, to some extent, a local redistribution of the settlements. This period not only brusquely interrupted the initial Neolithic diffusion but also marked a turning point of settlement size, density, and modes of production. From 5500 cal. BP onward, together with the return of land-use indicators in the palynological diagram of Pego-Oliva, the Neolithic IIB displayed a boom in population and economic intensification. Regional-scale occupation intensity, even if it cannot be surely interpreted in terms of population dynamics based on the radiocarbon record alone, is characterized here by the parallel increase of the number of the settlements and the area of these settlements (Figure 6). These processes were noticeably illustrated by the increasing use of silos, emblematic Neolithic storage pits for cereal and legume seeds [9].

5.3. Mid-Holocene Forest Demise During the Chalcolithic and the Bronze Age (5300–3200 cal. BP)

The Mid-Holocene forest demise is documented in two steps: affecting mesic vegetation to the benefit of sclerophyllous scrubs and maquia taxa (Pollen zone B2a, Figure 4) from 5300 cal. BP and culminating at the transition to the Late Holocene (Figure 6). This major vegetation rehearsal is documented over the Mediterranean Iberia, typically associated with the aridification of the Late Holocene climate in the Western Mediterranean [6], where drylands were converted to arid lands [21,62,82]. The high concentration of Pseudoschizaea also indicates the existence of seasonal desiccation in the Pego-Oliva record [14,62,83], explaining the decline of pollen concentration. In this context, fire, characterized in Pego-Oliva by a modest enhancement of small-size particles, was likely an additional important driver of instability at the regional-scale, precipitating the Mid-Holocene vegetation turnover [84]. Geomorphic archives located in the southern part of the Nao Cap [85]

supported a major change in the paleohydrological balance, showing a transition from long-term alluvial aggradation of the valley bottom from the Early to Mid-Holocene, shifting at about 5000 cal. BP to more instability, alternating phases of incision and aggradation.

This period coincided with a phase of intense soil erosion (higher MS values, peaks of Asteraceae, and other soil erosion indicators in Figure 4), occurring in the context of repeated evidence of agricultural (Cerealia-t) and pastoral activities (coprophilous spores and *Plantago*). Those activities taking place along the coast were likely part of a larger subsistence system (Figure 6), with the exploitation of inland forests that brought the dismantling of the mesophilic forests forward. Anthracological diagrams highlight these littoral/inland specificities: the coastal site of Cova de les Cendres shows dominance of *Pinus halepensis*, *Cistus*, *Erica multiflora*, and *Rosmarinus officinalis* [86], while for Niuet and Jovades, sites situated in interior valleys of the Nao Cap at ~400 m a.s.l., the assemblages turned to evergreen oak dominance [18,19]. Apart from the vegetation, other archeological evidence suggested a demographic boom [12,87] at that period associated with fundamental socio-economic transformations [88]. From the mid-IV millennium BC to the mid-III millennium we witnessed a process of progressive demographic expansion, and then the concentration in some places until the beginning of Bell Beaker period [89]. This process coincides with important economic changes in the agropastoral system and the development of extensive social networks through which diffuse products (like ivory, and copper), ideas (like maritime and international bell beaker styles) and maybe people. At local and regional-scale, sites such as Jovades, Arenal de la Costa, and La Vital [90] (i.e., this latter is close to Pego-Oliva), exemplify changes operating alongside these transformations. The use of oxen for traction plough could probably be placed from the beginning of this period, but the first direct dated bone with pathologies related to this activity comes from the site of Niuet at ca. 5200 cal. BP [91,92]. Moreover, the kill-off patterns of ovicaprine livestock in Arenal de la Costa [93] shows management centered in the caprine exploitation to obtain milk and derivates.

In the course of this period, the ~4.2 kyr cal. BP climate event [79] was likely expressed by drier hydrological conditions in the Western Mediterranean [94–97], in the context of high river alluviation [98] and more frequent summer rainfall [99]. Regarding the variety of the proxies, this climate event was likely a centennial-scale exacerbation of the Mediterranean climate, meaning a stronger seasonality of temperatures and precipitations [97]. In addition to presenting evidence of a drying out of the wetland and strong erosion, the Pego-Oliva record was characterized by irregular evidence of cereal cultivation and the absence of spores associated with livestock dung (Figure 4). This erosion dynamic was likely to result in a drying event, dismantling soils previously affected by anthropogenic activities [99]. A period of fewer archeological findings associated with the reduction of the size of the enclosures (Figure 6) was observed around 4200 cal. BP [12], which certain authors have connected, with caution, to a crisis of the Copper Age societies [100,101].

5.4. Xerophilous Vegetation Turnover from Late Bronze to Iron Age (3200–2000 cal. BP)

The process that started in the transition to the Late Holocene is documented until the end of the sequence (ca. 2000 cal. BP) with a predominance of the sclerophyllous vegetation (*Q. ilex-coccifera*, *Olea*, *Phillyrea*) at a regional scale (Pollen zone B2b, Figure 4). Sclerophyllous taxa (e.g., Ericaceae) markedly decreased, while *Juniperus*, *Tamarix*, and *Artemisia* increased, signalling an open vegetation turnover that led to the dominance of xerophilous scrubs [102], and no soil erosion was documented. This vegetation turnover was again accompanied by a minor increase in the long-distance charcoal record suggesting that those processes occurred more at a regional than at a local scale, and likely reflect the much lower biomass that was available, compared with earlier during the Mid-Holocene turnover [84]. In Pego-Oliva, the Bullent river mouth was characterized by a return of riparian vegetation (e.g., *Alnus*, *Fraxinus* in Figure 3A) with high values of hygrophilous plants, Characeae, *Gloeotrichia*, and HdV-128 (aquatic organisms with an affinity for carbonated marl substrates), indicating a significant renewal of the wetland waters, likely due to the perennial activity of the springs. The reactivation of springs was also noticed in the inland pollen record of Salines in this period [103].

Very little evidence of agriculture (Cerealia-t) and pasture lands (coprophilous fungi and ruderals *Galium*-t, *Rumex*, and *Plantago*) was recorded from 3200 to 2700 cal. BP (Figure 6). The Pego environmental record thus supports the apparent cessation of occupation of the valley suggested by the near absence of archeological evidence of the Final Bronze Age, which favored the overall vegetal reconquest at the landscape scale. This period also strikingly corresponded to a regional-climate event (~2.8 kyr BP event, during the period 3400–2800 cal. BP [79]) that had known repercussions in the Mediterranean Iberia, likely characterized by drier conditions [102].

Finally, evidence of land use reappeared with the development of the Iron Age hillforts from 2720–2425 cal. BP onward (Figure 6), as was dated in L'Alt Benimaquia [104], and the introduction of a more diversified economy of food production, in particular the viniculture and arboriculture. In the Pego valley, the Middle Iberian and Ibero-Roman implantations (e.g., Passet de Segaria, El Castellar, and Tossalet de les Mondes [105–107], Figure 5) were likely part of a single consolidated territory relying on the agrarian economy [78], which related well to the combined reoccurrence of the agricultural and pastoral indicators (Figure 6) from 2700 to 2200 cal. BP.

6. Conclusions

The continuous sedimentological and palynological records obtained in a sheltered geomorphological position to the marine processes of the plain of Pego-Oliva allowed us to decipher the coastal paleoenvironmental and anthropogenic dynamics during the Middle and the Late Holocene, from ca. 7000 to 2000 cal. BP, in the south-western Mediterranean. First, regarding the paleoenvironmental record, both the local (i.e., the littoral fringe) and regional scale (i.e., inner valleys) were registered, allowing us to:

1. characterize the Mid-Holocene Climatic Optimum of the mesophilous oak forest that developed in the inner valley from the beginning of the sequence to 5300 cal. BP, confirmed by comparisons conducted with anthracological records from the archeological sites;
2. underline the role of fire in the vegetation turnover at 5300 cal. BP (i.e., mixed oak forests replaced by sclerophyllous trees and matorral scrubs) and at 3200 cal. BP (i.e., the dominance of xerophytics);
3. show the variability of karst spring outflow influencing the wetland ecology, with phases of fresh running water at 7000–6000 and 3200–2000 cal. BP, a pseudo-lacustrine freshwater phase (6000–5300 cal. BP), and a phase of desiccation (5300–3200 cal. BP) reaching a maximum at ~4200 cal. BP; and
4. provide evidence of one short soil erosion event occurring at ca. 5900 cal. BP that likely relates to the lower level of vast coalescent dejection fans [33], and one long-lasting phase covering the period 5200–3800 cal. BP, that corresponds to the permanency of the agropastoral practices in the littoral hills.

Second, regarding the anthropogenic record, we reconstructed a chronicle of the agricultural practices (i.e., the presence of Cerealia-t pollen grains) and animal husbandry (i.e., the presence of coprophilous fungi spores, interpreted with the ruderal herbaceous cortege in the most recent periods (*Galium, Rumex*, and *Plantago*). Our study demonstrated that:

1. Agriculture and animal husbandry were common practices in this littoral area 7000 years ago, a fact confirmed by the archeological record. Indeed, the littoral of the Nao Cap is, to date, the oldest evidence of Neolithic settlement and culture diffusion inland in the Iberian Peninsula.
2. The gaps of agropastoral indicators were very consistent to the local- and regional-scale archeological record (i.e., hiatus of occupations at the Mid- to Late Neolithic transition and Final Bronze Age, and a near cessation of the occupations at the end of the Chalcolithic), underlining the importance of considering the socio-ecological systems as a whole.
3. Breakdowns in the socio-ecological trajectory matched three short-term climate events at ~5.9, ~4.2, and ~2.8 kyr BP, known to have affected the North Atlantic, and likely expressed as an

accentuation of the aridity in the Iberian Peninsula. Water scarcity was likely a key cause of land abandonment; however, this interpretation was supported for the 4.2 and 2.8 kyr BP events only.

Far from interpretation as simple causal links, this pleads for a contingency of the socio-ecosystem trajectories with global climate changes [108], given their co-construction over millennia. In more general terms, this case study, covering several millennia and three abrupt climate events, highlights how climate change (specifically drought and its consequences on water availability) affected prehistoric communities (i.e., abandoning formerly exploited lands) and also demonstrated that people repeatedly reinstalled their activities near the coast once the perturbation was gone. This indicates that often, for societies, the attractiveness of an environment goes beyond climatic hazard exposure.

Author Contributions: Conceptualization and funding, E.B. and F.B.; analyses, E.B., J.R., and I.E.; original draft preparation, E.B and J.R.; multiproxy interpretation, E.B. and J.B.A.; editing and final review, all the authors. All authors have read and agreed to the published version of the manuscript.

Funding: The data were obtained in the frame of the project MedCoRes (704822) led by E.B., funded by the Marie Sklodowska-Curie Actions (European Commission). E.B. is supported by the foundation "La Caixa" (LCF/BQ/PR19/11700001), F.B. benefits from a MINECO grant (HAR2017-88503-P) and J.R. from a Juan de la Cierva grant (FJC2017). E.B, J.R., I.E., and F.B. were members of the SGR n°836 (AGAUR).

Acknowledgments: The authors kindly acknowledge Cristina Val-Peón (Univ. Aachen) for providing assistance, the GRC Marine Geosciences (Univ. Barcelona) for magnetic susceptibility analysis, and the three anonymous reviewers that helped to finalize the manuscript.

Conflicts of Interest: The authors declare no conflict of interest. The funders had no role in the design of the study, the interpretation of data, the writing of the manuscript, or the decision to publish the results.

References

1. Erlandson, J.M. The Archaeology of Aquatic Adaptations: Paradigms for a New Millennium. *J. Archaeol. Res.* **2001**, *9*, 287–350. [CrossRef]
2. Manen, C. Spatial, chronological and cultural dynamics of the neolithization in the Western Mediterranean. In *The Neolithic transition in the Mediterranean*; Manen, C., Perrin, T., Guilaine, J., Eds.; Errance/AEP: Paris, France, 2014; pp. 405–418.
3. García-Puchol, O.; Diez Castillo, A.A.; Pardo-Gordó, S. Timing the Western Mediterranean Last Hunter-Gatherers and First Farmers. In *Times of Neolithic Transition along the Western Mediterranean, Fundamental Issues in Archaeology*; García-Puchol, O., Salazar-García, D.C., Eds.; Springer International Publishing: Berlin/Heidelberg, Germany, 2017; pp. 69–99. [CrossRef]
4. Zapata, L.; Peña-Chocarro, L.; Pérez-Jordá, G.; Stika, H.-P. Early Neolithic Agriculture in the Iberian Peninsula. *J. World Prehist.* **2004**, *18*, 283–325. [CrossRef]
5. Antolín, F.; Jacomet, S.; Buxó, R. The hard knock life. Archaeobotanical data on farming practices during the Neolithic (5400–2300 cal BC) in the NE of the Iberian Peninsula. *J. Archaeol. Sci.* **2015**, *61*, 90–104. [CrossRef]
6. Roberts, C.N.; Woodbridge, J.; Palmisano, A.; Bevan, A.; Fyfe, R.; Shennan, S. Mediterranean landscape change during the Holocene: Synthesis, comparison and regional trends in population, land cover and climate. *Holocene* **2019**, *29*, 923–937. [CrossRef]
7. Van de Noort, R. Conceptualising climate change archaeology. *Antiquity* **2011**, *85*, 1039–1048. [CrossRef]
8. Bernabeu, J.; Molina, L. *La Cova de Les Cendres*; Serie Mayor 6; Fundación MARQ: Alicante, Spain, 2009; p. 236.
9. Bernabeu Aubán, J.; Jiménez-Puerto, J.; Escriba Ruiz, P.; Pardo-Gordó, S. C14 y Poblamiento en las Comarcas Centro-Meridionales del País Valenciano (c. 7000–1500 cal BC). *Recer. Mus. D'Alcoi* **2018**, *27*, 35–48.
10. García-Puchol, O.; Aura Tortosa, J.E. *El Abric de la Falguera (Alcoi, Alacant): 8.000 Años de Ocupación Humana en la Cabecera del Río de Alcoi*; Museu arqueologic municipal d'Alcoi: Alcoy, Spain, 2006; p. 301.
11. Bernabeu Aubán, J.; Manen, C.; Pardo-Gordó, S. Spatial and Temporal Diversity During the Neolithic Spread in the Western Mediterranean: The First Pottery Productions. In *Times of Neolithic Transition along the Western Mediterranean, Fundamental Issues in Archaeology*; García-Puchol, O., Salazar-García, D.C., Eds.; Springer Publishing: Berlin/Heidelberg, Germany, 2017; pp. 373–397. [CrossRef]
12. Balsera, V.; Aubán, J.B.; Costa-Caramé, M.; Díaz-del-Río, P.; Sanjuán, L.G.; Pardo, S. The Radiocarbon Chronology of Southern Spain's Late Prehistory (5600–1000 cal BC): A Comparative Review. *Oxf. J. Archaeol.* **2015**, *34*, 139–156. [CrossRef]

13. Jiménez-Puerto, J.; Bernabeu Aubán, J.; Orozco, T. Habitat evolution in Iberian Eastern façade, from Neolithic to the Bronze Age. In *Reactive Proactive, Architecture*; University Politècnica València: Valencia, Spain, 2018; pp. 138–143.
14. Carrión, J.S.; Navarro, C. Cryptogam spores and other non-pollen microfossils as sources of palaeoecological information: Case-studies from Spain. *Ann. Bot. Fenn.* **2002**, *39*, 1–14.
15. Pérez-Jordà, G.; Peña-Chocarro, L. Agricultural production between the 6th and the 3rd millennium cal BC in the central part of the Valencia region (Spain). In *Barely Surviving or More than Enough? The Environmental Archaeology of Subsistence, Specialisation and Surplus Food Production*; Groot, M., Lentjes, D., Zeiler, J., Eds.; Sidestone Press: Leiden, The Netherlands, 2013; pp. 81–100.
16. Bernabeu Aubán, J.; Michael Barton, C.; Pardo Gordó, S.; Bergin, S.M. Modeling initial Neolithic dispersal. The first agricultural groups in West Mediterranean. *Ecol. Model.* **2015**, *307*, 22–31. [CrossRef]
17. Mercuri, A.M.; Florenzano, A.; Burjachs, F.; Giardini, M.; Kouli, K.; Masi, A.; Picornell-Gelabert, L.; Revelles, J.; Sadori, L.; Servera-Vives, G.; et al. From influence to impact: The multifunctional land use in Mediterranean prehistory emerging from palynology of archaeological sites (8.0–2.8 ka BP). *Holocene* **2019**, *29*, 830–846. [CrossRef]
18. Badal, E.; Bernabeu Aubán, J.; Vernet, J.L. Vegetation changes and human action from the Neolithic to the Bronze Age (7000–4000 B.P.) in Alicante, Spain, based on charcoal analysis. *Veg. Hist. Archaeobot.* **1994**, *3*, 155–166. [CrossRef]
19. Bernabeu Aubán, J.; Badal, E. A view of the vegetation and economic exploitation of the forest in the Late Neolithic sites of Les Jovades and Niuet (Alicante, Spain). *Bull. Soc. Bot. Fr.* **1992**, *139*, 697–714. [CrossRef]
20. Bernabeu Aubán, J.; Orozco-Köhler, T.; Diez Castillo, A.A.; Gómez Puche, M.; Molina Hernández, F.J. Mas d'Is (Penàguila, Alicante): Aldeas y recintos monumentales del Neolítico Inicial en el valle del Serpis. *Trab. Prehist.* **2003**, *60*, 39–59. [CrossRef]
21. Carrión, J.S.; Fernández, S.; González-Sampériz, P.; Gil-Romera, G.; Badal, E.; Carrión-Marco, Y.; López-Merino, L.; López-Sáez, J.A.; Fierro, E.; Burjachs, F. Expected trends and surprises in the Lateglacial and Holocene vegetation history of the Iberian Peninsula and Balearic Islands. *Rev. Palaeobot. Palynol.* **2010**, *162*, 458–475. [CrossRef]
22. Carrión, J.S. *Paleoflora y Paleovegetación de la Península Ibérica e Islas Baleares*; Universidad de Murcia: Murcia, Spain, 2012; p. 994.
23. Planchais, N.; Parra, I. Analyses polliniques de sédiments lagunaires et côtiers en Languedoc, en Roussillon et dans la province de Castellón (Espagne); Bioclimatologie. *Bull. Soc. Bot. Fr.* **1984**, *131*, 97–105. [CrossRef]
24. Marco-Barba, J.; Burjachs, F.; Reed, J.M.; Santisteban, C.; Usera, J.M.; Alberola, C.; Expósito, I.; Guillem, J.; Patchett, F.; Vicente, E.; et al. Mid-Holocene and historical palaeoecology of the Albufera de València coastal lagoon. *Limnetica* **2019**, *38*, 353–389. [CrossRef]
25. Dupré, M.; Fumanal, M.P.; Sanjaume, E.; Santisteban, C.; Usera, J.; Viñals, M.J. Quaternary evolution of the Pego coastal lagoon (Southern Valencia, Spain). *Palaeogeogr. Palaeoclimatol. Palaeoecol.* **1988**, *68*, 291–299. [CrossRef]
26. Viñals, M.J.; Belluomini, G.; Fumanal, M.P.; Dupré, M.; Usera, J.; Mestres, J.; Manfra, L. Rasgos paleoambientales holocenos en la Bahía de Xàbia (Alicante). In *Estudios Sobre Cuatern*; Fumanal, M.P., Bernabeu, J., Eds.; Universitat de Valencia: Valencia, Spain, 1993; pp. 107–114.
27. Court-Picon, M.; Vella, C.; Chabal, L.; Bruneton, H. Paléo-environnements littoraux depuis 8000 ans sur la bordure occidentale du Golfe du Lion. Le lido de l'Etang de Thau (carottage SETIF, Sète, Hérault). *Quaternaire* **2010**, *21*, 43–60. [CrossRef]
28. Devillers, B.; Bony, G.; Degeai, J.-P.; Gascò, J.; Lachenal, T.; Bruneton, H.; Yung, F.; Oueslati, H.; Thierry, A. Holocene coastal environmental changes and human occupation of the lower Hérault River, southern France. *Quat. Sci. Rev.* **2019**, *222*, 105912. [CrossRef]
29. Melis, R.T.; Di Rita, F.; French, C.; Marriner, N.; Montis, F.; Serreli, G.; Sulas, F.; Vacchi, M. 8000 years of coastal changes on a western Mediterranean island: A multiproxy approach from the Posada plain of Sardinia. *Mar. Geol.* **2018**, *403*, 93–108. [CrossRef]
30. Poher, Y.; Ponel, P.; Médail, F.; Andrieu-Ponel, V.; Guiter, F. Holocene environmental history of a small Mediterranean island in response to sea-level changes, climate and human impact. *Palaeogeogr. Palaeoclimatol. Palaeoecol.* **2017**, *465*, 247–263. [CrossRef]

31. Revelles, J.; Ghilardi, M.; Rossi, V.; Currás, A.; López-Bultó, O.; Brkojewitsch, G.; Vacchi, M. Coastal landscape evolution of Corsica island (W. Mediterranean): Palaeoenvironments, vegetation history and human impacts since the early Neolithic period. *Quat. Sci. Rev.* **2019**, *225*, 105993. [CrossRef]
32. Ejarque, A.; Julià, R.; Reed, J.M.; Mesquita-Joanes, F.; Marco-Barba, J.; Riera, S. Coastal Evolution in a Mediterranean Microtidal Zone: Mid to Late Holocene Natural Dynamics and Human Management of the Castelló Lagoon, NE Spain. *PLoS ONE* **2016**, *11*, e0155446. [CrossRef]
33. Brisset, E.; Burjachs, F.; Ballesteros Navarro, B.J.; de Pablo, J.F.L. Socio-ecological adaptation to Early-Holocene sea-level rise in the western Mediterranean. *Glob. Planet. Chang.* **2018**, *169*, 156–167. [CrossRef]
34. Planchais, N. Palynologie lagunaire: L'exemple du Languedoc-Roussillon. *Ann. Géogr.* **1984**, *93*, 268–275.
35. Fumanal, M.P.; Mateu, G.; Rey, J.; Somoza, L.; Viñals, M.J. Las unidades morfosedimentarias cuaternarias del litoral del Cap de la Nau (Valencia-Alicante) y su correlación con la plataforma continental. In *Estudios Sobre Cuatern*; Fumanal, M.P., Bernabeu, J., Eds.; Universitat de Valencia: Valencia, Spain, 1993; pp. 53–64.
36. Anthony, E.J.; Marriner, N.; Morhange, C. Human influence and the changing geomorphology of Mediterranean deltas and coasts over the last 6000years: From progradation to destruction phase? *Earth-Sci. Rev.* **2014**, *139*, 336–361. [CrossRef]
37. Fumanal, M.P.; Viñals, M.J.; Ferrer, C.; Aura, E.; Bernabeu, J.; Casabó, J.; Gisbert, J.; Sentí, M.A. Litoral y poblamiento en el litoral valenciano durante el Cuaternario reciente: Cap de Cullera-Puntal de Moraira. In *Estudios Sobre Cuatern*; Fumanal, M.P., Bernabeu, J., Eds.; Universitat de Valencia: Valencia, Spain, 1993; pp. 249–259.
38. Viñals, M.J.; Fumanal, M.P. Quaternary development and evolution of the sedimentary environments in the Central Mediterranean Spanish coast. *Quat. Int.* **1995**, *29*, 119–128. [CrossRef]
39. Carmona, P.; Ruiz, J.M. Historical morphogenesis of the Turia River coastal flood plain in the Mediterranean littoral of Spain. *CATENA* **2011**, *86*, 139–149. [CrossRef]
40. Carmona, P.; Ruiz-Pérez, J.-M.; Blázquez, A.-M.; López-Belzunce, M.; Riera, S.; Orengo, H. Environmental evolution and mid–late Holocene climate events in the Valencia lagoon (Mediterranean coast of Spain). *Holocene* **2016**, *26*, 1750–1765. [CrossRef]
41. Rey, J.; Fumanal, P.M. The Valencian coast (Western Mediterranean): Neotectonics and geomorphology. *Quat. Sci. Rev.* **1996**, *15*, 789–802. [CrossRef]
42. Ballesteros Navarro, B.; Domínguez Sánchez, J.A.; Díaz-Losada, E.; García Menéndez, O. Zonas húmedas mediterráneas y acuíferos asociados. Condicionantes hidrogeológicos del Marjal de Pego-Oliva (Alicante-Valencia). *Bol. Geo. Min.* **2009**, *120*, 459–478.
43. Cirujano, S.; Medina, L.; Peris, J.B.; Stübing, G. Estudio de la Flora y Vegetacion de las Marjales de Pego-Oliva y la Safor Orientado a su Gestion, Valencia, Spain. 1995, p. 284. Available online: http://www.humedalesibericos.com/sesiones/humedales1/web/publicaciones/sp_35.pdf (accessed on 3 July 2020).
44. Rivas-Martínez, S.; Penas, Á.; Díaz González, T.E.; Cantó, P.; del Río, S.; Costa, J.C.; Herrero, L.; Molero, J. Biogeographic Units of the Iberian Peninsula and Baelaric Islands to District Level. A Concise Synopsis. In *The Vegetation of the Iberian Peninsula*; Loidi, J., Ed.; Plant and Vegetation; Springer Publishing: Berlin/Heidelberg, Germany, 2017; Volume 1, pp. 131–188. [CrossRef]
45. Soriano, P.; Costa, M. The Coastal Levantine Area. In *The Vegetation of the Iberian Peninsula*; Loidi, J., Ed.; Plant and Vegetation; Springer Publishing: Berlin/Heidelberg, Germany, 2017; Volume 1, pp. 589–625.
46. Reimer, P.J.; Bard, E.; Bayliss, A.; Beck, J.W.; Blackwell, P.G.; Ramsey, C.B.; Buck, C.E.; Cheng, H.; Edwards, R.L.; Friedrich, M.; et al. IntCal13 and Marine13 Radiocarbon Age Calibration Curves 0–50,000 Years cal BP. *Radiocarbon* **2013**, *55*, 1869–1887. [CrossRef]
47. Blaauw, M. Methods and code for 'classical' age-modelling of radiocarbon sequences. *Quat. Geochronol.* **2010**, *5*, 512–518. [CrossRef]
48. Nowaczyk, N.R. Logging of Magnetic Susceptibility. In *Tracking Environmental Change Using Lake Sediments: Basin Analysis, Coring, and Chronological Techniques, Developments in Paleoenvironmental Research*; Last, W.M., Smol, J.P., Eds.; Springer: Dordrecht, The Netherlands, 2001; pp. 155–170. [CrossRef]
49. Whitlock, C.; Larsen, C. Charcoal as a fire proxy. In *Tracking Environmental Change Using Lake Sediments: Terrestrial, Algal, and Siliceous Indicators*; Last, W.M., Smol, J.P., Eds.; Springer: Dordrecht, The Netherlands, 2001; pp. 75–97. [CrossRef]
50. Goeury, C.; De Beaulieu, J.L. À propos de la concentration du pollen à l'aide de la liqueur de Thoulet dans les sédiments minéraux. *Pollen Spores* **1979**, *XXI*, 239–251.

51. Girard, M. Nouvelles techniques de préparation en palynologie appliqués à trois sédiments du Quaternaire final de l'Abri Cornille (Istres -Bouches du Rhône). *Quaternaire* **1969**, *6*, 275–278. [CrossRef]
52. Reille, M. *Pollen et Spores d'Europe et d'Afrique du Nord*; Laboratoire de Botanique Historique et Palynologie Editions: Marseille, France, 1992; p. 543.
53. Faegri, K.; Iversen, J. *Textbook of Pollen Analysis*; John Wiley & Sons: Chichester, UK, 1989; p. 328.
54. Van Geel, B.; Buurman, J.; Brinkkemper, O.; Schelvis, J.; Aptroot, A.; van Reenen, G.; Hakbijl, T. Environmental reconstruction of a Roman Period settlement site in Uitgeest (The Netherlands), with special reference to coprophilous fungi. *J. Archaeol. Sci.* **2003**, *30*, 873–883. [CrossRef]
55. Revelles, J.; Burjachs, F.; van Geel, B. Pollen and non-pollen palynomorphs from the Early Neolithic settlement of La Draga (Girona, Spain). *Rev. Palaeobot. Palynol.* **2016**, *225*, 1–20. [CrossRef]
56. Revelles, J.; van Geel, B. Human impact and ecological changes in lakeshore environments. The contribution of non-pollen palynomorphs in Lake Banyoles (NE Iberia). *Rev. Palaeobot. Palynol.* **2016**, *232*, 81–97. [CrossRef]
57. Grimm, E.C. CONISS: A FORTRAN 77 program for stratigraphically constrained cluster analysis by the method of incremental sum of squares. *Comput. Geosci.* **1987**, *13*, 13–35. [CrossRef]
58. Grimm, E.C. *Tilia, Tilia-Graph and TGView*; Illinois State Museum: Springfield, IL, USA, 1991; Available online: https://www.tiliait.com/ (accessed on 3 July 2020).
59. Gelorini, V.; Verbeken, A.; van Geel, B.; Cocquyt, C.; Verschuren, D. Modern non-pollen palynomorphs from East African lake sediments. *Rev. Palaeobot. Palynol.* **2011**, *164*, 143–173. [CrossRef]
60. Torres, T.; Ortiz, J.E.; Martín-Sánchez, D.; Arribas, I.; Moreno, L.; Ballesteros, B.; Blázquez, A.; Domínguez, J.A.; Estrella, T.R. The long Pleistocene record from the Pego-Oliva marshland (Alicante-Valencia, Spain). *Geol. Soc.* **2014**, *388*, 429–452. [CrossRef]
61. Vacchi, M.; Ghilardi, M.; Melis, R.T.; Spada, G.; Giaime, M.; Marriner, N.; Lorscheid, T.; Morhange, C.; Burjachs, F.; Rovere, A. New relative sea-level insights into the isostatic history of the Western Mediterranean. *Quat. Sci. Rev.* **2018**, *201*, 396–408. [CrossRef]
62. Carrión, J.S.; Fierro, E.; Ros, M.; Munuera, M.; Fernández, S.; Ochando, J.; Amorós, G.; Navarro, F.; Rodríguez-Estrella, T.; Manzano, S.; et al. Ancient Forests in European drylands: Holocene palaeoecological record of Mazarrón, south-eastern Spain. *Proc. Geol. Asso.* **2018**, *129*, 512–525. [CrossRef]
63. Court-Picon, M.; Buttler, A.; de Beaulieu, J.-L. Modern pollen/vegetation/land-use relationships in mountain environments: An example from the Champsaur valley (French Alps). *Veg. Hist. Archaeobot.* **2006**, *15*, 151–168. [CrossRef]
64. Deza-Araujo, M.; Morales-Molino, C.; Tinner, W.; Henne, P.D.; Heitz, C.; Pezzatti, G.B.; Hafner, A.; Conedera, M. A critical assessment of human-impact indices based on anthropogenic pollen indicators. *Quat. Sci. Rev.* **2020**, *236*, 106291. [CrossRef]
65. Bernabeu Aubán, J.; Martí, B. The first agricultural groups in the Iberian Peninsula. In *La Transition Néolithique en Méditerranée*; Errance Publishing: Paris, France, 2014; pp. 419–438.
66. Bernabeu Aubán, J.; Molina, L.L.; Esquembre-Bebiá, M.A.; Ortega, J.R.; Boronat, J. La cerámica impresa mediterránea en el origen del Neolítico de la península ibérica. In *De Méditerranée et D'ailleurs. Mélanges Offerts à J. Guilaine*; Les Archives d'Ecologie Préhistorique: Toulouse, France, 2009; pp. 83–95.
67. Pantaléon-Cano, J.; Yll, E.-I.; Pérez-Obiol, R.; Roure, J.M. Palynological evidence for vegetational history in semi-arid areas of the western Mediterranean (Almería, Spain). *Holocene* **2003**, *13*, 109–119. [CrossRef]
68. Carrión, J.S.; Fernández, S.; Jiménez-Moreno, G.; Fauquette, S.; Gil-Romera, G.; González-Sampériz, P.; Finlayson, C. The historical origins of aridity and vegetation degradation in southeastern Spain. *J. Arid Environ.* **2010**, *74*, 731–736. [CrossRef]
69. Carrión, J.S.; Van Geel, B. Fine-resolution Upper Weichselian and Holocene palynological record from Navarrés (Valencia, Spain) and a discussion about factors of Mediterranean forest succession. *Rev. Palaeobot. Palynol.* **1999**, *106*, 209–236. [CrossRef]
70. Carrión-Marco, Y. *La Vegetación Mediterránea y Atlántica de la Península Ibérica: Nuevas Secuencias Antracológicas*; Servicio de Investigación Prehistórica: Valencia, Spain, 2005; p. 314.
71. López Sáez, J.A.; Van Geel, B.; Sánchez, M.M. Aplicación de los microfósiles no polínicos en Palinología Arqueológica. In *Congresso de Arqueologia Peninsular*; ADECAP: Vila Real, Portugal, 2000; pp. 11–20.

72. Esquembre-Bebiá, M.A.; Soler, J.D.D.B.; Maestre, F.J.J.; Hernández, F.J.M.; Navas, A.L.; de Pablo, J.F.L.; Valle, R.M.; Eres, M.P.I.; García, C.F.; Pastor, R.R.; et al. El yacimiento neolítico del Barranquet de Oliva (Valencia). In *IV Congreso del Neolítico Peninsular*; Museo Arqueológico Alicante: Alicante, Spain, 2008; pp. 183–190.
73. Bernabeu Aubán, J.; Molina, L.; Diez, A.; Orozco, T. Inequalities and Power. Three Millennia of Prehistory in Mediterranean Spain (5600—2000 cal BC). In *Social Inequality in Iberian Late Prehistory*; BAR International Series; Archaeopress: Oxford, UK, 2006; pp. 97–116.
74. Miquel Calatayud, P.; Guitart Perarnau, I.; Martinez Valle, R.; Mata Parreño, C.; Pascual Benito, J.L. *L'ocupació Prehistòrica de la Cova de Bolumini (Beniarbeig-Benimeli-Marina Alta)*; Actes del III Congres de Història de la Marina Alta; Institut d'Estudis Comarcals de la Marina Alta: Pedreguer, Spain, 1992; pp. 31–48.
75. Alonso López, A.M. Las dinámicas de poblamiento ibérico y romano en la Vall d'Albaida, L'Alcoià y El Comtat (ss. IV a.C.-II d.C.): Un estudio comparativo del patrón de asentamiento. *Recer. Mus. D'Alcoi* **2018**, *27*, 63–78.
76. García Atiénzar, G.; Barciela González, V. La Prehistòria a la Marina Alta (Alacant): De Les Primeres Poblacions Humanes al Final de L'Edat del Bronze. In *VI Jornades d'Estudis Carmel Giner Bolufer de Pego i Les Valls Actes*; De Pego, A., Ed.; Institut d'Estudis Comarcals de la Marina Alta: Pego, Spain, 2018; pp. 103–114.
77. Grau Mira, I. El Poblamiento de Época Ibérica en la Region Centro-Meridional del País Valenciano. Ph.D. Thesis, Universidad de Alicante, Alicante, Spain, 2000; p. 524.
78. Grau Mira, I. Les Valls de Pego en el Marc del Paisatge Ibèric de la Marina Alta (Segles vii-ii a.n.e.). In *VI Jornades d'Estudis Carmel Giner Bolufer de Pego I Les Valls Actes*; De Pego, A., Ed.; Institut d'Estudis Comarcal de la Marina Alta: Pego, Spain, 2018; pp. 111–128.
79. Bond, G.; Kromer, B.; Beer, J.; Muscheler, R.; Evans, M.N.; Showers, W.; Hoffmann, S.; Lotti-Bond, R.; Hajdas, I.; Bonani, G. Persistent Solar Influence on North Atlantic Climate During the Holocene. *Science* **2001**, *294*, 2130–2136. [CrossRef]
80. Aparicio, J.; Climent, S. Sobre la pesca en la edad del bronce. *ARSE* **1985**, *20*, 481–485.
81. Bernabeu Aubán, J.; García Puchol, O.; Barton, C.M.; McClure, S.; Pardo Gordó, S. Radiocarbon dates, climatic events, and social dynamics during the Early Neolithic in Mediterranean Iberia. *Quat. Int.* **2016**, *403*, 201–210. [CrossRef]
82. Schröder, T.; van't Hoff, J.; López-Sáez, J.A.; Viehberg, F.; Melles, M.; Reicherter, K. Holocene climatic and environmental evolution on the southwestern Iberian Peninsula: A high-resolution multi-proxy study from Lake Medina (Cádiz, SW Spain). *Quat. Sci. Rev.* **2018**, *198*, 208–225. [CrossRef]
83. Scott, L. Environmental implications and origin of microscopic Pseudoschizaea Thiergart and Frantz ex R. Potonié emend. in sediments. *J. Biogeogr.* **1992**, *19*, 349–354. [CrossRef]
84. Connor, S.E.; Vannière, B.; Colombaroli, D.; Anderson, R.S.; Carrión, J.S.; Ejarque, A.; Romera, G.G.; González-Sampériz, P.; Hoefer, D.; Morales-Molino, C.; et al. Humans take control of fire-driven diversity changes in Mediterranean Iberia's vegetation during the mid–late Holocene. *Holocene* **2019**, *29*, 886–901. [CrossRef]
85. Rodriguez-Lloveras, X.; Machado, M.J.; Sanchez-Moya, Y.; Calle, M.; Medialdea, A.; Sopeña, A.; Benito, G. Impacts of sediment connectivity on Holocene alluvial records across a Mediterranean basin (Guadalentín River, SE-Spain). *CATENA* **2020**, *187*, 104321. [CrossRef]
86. Badal, E. Estudio antracológico de la secuencia holocena de la Cova de les Cendres. In *La Cova de Les Cendres: (Moraira-Teulada, Alicante)*; Museo Arqueológico de Alicante-MARQ: Alicante, Spain, 2009; pp. 125–134.
87. Fyfe, R.M.; Woodbridge, J.; Palmisano, A.; Bevan, A.; Shennan, S.; Burjachs, F.; Legarra Herrero, B.; García Puchol, O.; Carrión, J.-S.; Revelles, J.; et al. Prehistoric palaeodemographics and regional land cover change in eastern Iberia. *Holocene* **2019**, *29*, 799–815. [CrossRef]
88. Bernabeu Auban, J.; Moreno Martín, A.; Barton, C.M. Complex systems, social networks and the evolution of social complexity. In *The Prehistory of Iberia: Debating Early Social Stratification and the State*; Berrocal, M., García Sanjuán, L., Gilman, A., Eds.; Routledge: New York, NY, USA, 2012; pp. 23–37.
89. Knipper, C.; Rihuete-Herrada, C.; Voltas, J.; Held, P.; Lull, V.; Micó, R.; Risch, R.; Alt, K.W. Reconstructing Bronze Age diets and farming strategies at the early Bronze Age sites of La Bastida and Gatas (southeast Iberia) using stable isotope analysis. *PLoS ONE* **2020**, *15*, e0229398. [CrossRef]

90. García-Puchol, O.; Bernabeu Aubán, J.; Carrión, M.; Molina Balaguer, Y.; Perez Jorda, G.; Gómez Puche, M. A funerary perspective on Bell Beaker period in the Western Mediterranean. Reading the social context of individual burials at La Vital (Gandía, Valencia). *Trab. Prehist.* **2013**, *70*, 325–339. [CrossRef]
91. Bernabeu Aubán, J.; Pascual, J.L.; Orozco, T.; Badal, E.; Fumanal, M.P.; García Puchol, O. *Niuet (L'Alqueria d'Asnar). Poblado del III Milenio aC*; Museu d'Alcoi: Alcoy, Spain, 1994; pp. 9–74.
92. Murillo-Barroso, M.; Martinón-Torres, M.; Massieu, M.D.C.; Socas, D.M.; González, F.M. Early metallurgy in SE Iberia. The workshop of Las Pilas (Mojácar, Almería, Spain). *Archaeol. Anthropol. Sci.* **2017**, *9*, 1539–1569. [CrossRef]
93. Pérez Ripoll, M. La explotación ganadera durante el IIIr milenio aC en la Península Ibérica. In *II Congres del Neolític a la Península Ibèrica. SAGUNTUM*; Universitat de València: Valencia, Spain, 1999; Volume 2, pp. 95–103.
94. Ruan, J.; Kherbouche, F.; Genty, D.; Blamart, D.; Cheng, H.; Dewilde, F.; Hachi, S.; Edwards, R.L.; Régnier, E.; Michelot, J.-L. Evidence of a prolonged drought ca. 4200 yr BP correlated with prehistoric settlement abandonment from the Gueldaman GLD1 Cave, Northern Algeria. *Clim. Past* **2016**, *12*, 1–14. [CrossRef]
95. Bini, M.; Zanchetta, G.; Perşoiu, A.; Cartier, R.; Català, A.; Cacho, I.; Dean, J.R.; Rita, F.D.; Drysdale, R.N.; Finnè, M.; et al. The 4.2 ka BP Event in the Mediterranean region. *Clim. Past* **2019**, *15*, 555–577. [CrossRef]
96. Cartier, R.; Brisset, E.; Guiter, F.; Sylvestre, F.; Tachikawa, K.; Anthony, E.J.; Paillès, C.; Bruneton, H.; Bard, E.; Miramont, C. Multiproxy analyses of Lake Allos reveal synchronicity and divergence in geosystem dynamics during the Lateglacial/Holocene in the Alps. *Quat. Sci. Rev.* **2018**, *186*, 60–77. [CrossRef]
97. Cartier, R.; Sylvestre, F.; Paillès, C.; Sonzogni, C.; Couapel, M.; Alexandre, A.; Mazur, J.-C.; Brisset, E.; Miramont, C.; Guiter, F. Diatom-oxygen isotope record from high-altitude Lake Petit (2200 m a.s.l.) in the Mediterranean Alps: Shedding light on a climatic pulse at 4.2 ka. *Clim. Past* **2019**, *15*, 253–263. [CrossRef]
98. Brisset, E.; Miramont, C.; Anthony, E.J.; Bruneton, H.; Rosique, T.; Sivan, O. Sediment budget quantification of a sub-Alpine river catchment since the end of the last glaciation. *CATENA* **2014**, *114*, 169–179. [CrossRef]
99. Brisset, E.; Miramont, C.; Guiter, F.; Anthony, E.J.; Tachikawa, K.; Poulenard, J.; Arnaud, F.; Delhon, C.; Meunier, J.-D.; Bard, E.; et al. Non-reversible geosystem destabilisation at 4200 cal. BP: Sedimentological, geochemical and botanical markers of soil erosion recorded in a Mediterranean alpine lake. *Holocene* **2013**, *23*, 1863–1874. [CrossRef]
100. Lull, V.; Micó, R.; Rihuete, C.; Risch, R. Límites históricos y limitaciones del conocimiento arqueológico: La transición entre los grupos arqueológicos de Los Millares y El Argar. In *Arqueología, Sociedad, Territorio y Paisaje, Homenaje a D. Fernández Posse*; Bueno Ramírez, P., Ed.; Consejo Superior de Investigaciones Científicas, CSIC, Instituto de Historia: Madrid, Spain, 2010; pp. 75–94. Available online: https://www.torrossa.com/digital/fcov/2010/2471828_FCOV.pdf#page=73 (accessed on 3 July 2020).
101. Carozza, L.; Berger, J.F.; Burens-Carozza, A.; Marcigny, C. Society and environment in Southern France from the 3rd millennium BC to the beginning of the 2nd millennium BC: 2200 BC a tipping point? In Proceedings of the 7th Archaeological Conference of Central Germany, Halle, Germany, 23–26 October 2014; pp. 335–362. Available online: https://halshs.archives-ouvertes.fr/halshs-01245488/ (accessed on 3 July 2020).
102. Carrión, J.S.; Andrade, A.; Bennett, K.D.; Navarro, C.; Munuera, M. Crossing forest thresholds: Inertia and collapse in a Holocene sequence from south-central Spain. *Holocene* **2001**, *11*, 635–653. [CrossRef]
103. Burjachs, F.; Jones, S.E.; Giralt, S.; de Pablo, J.F.L. Lateglacial to Early Holocene recursive aridity events in the SE Mediterranean Iberian Peninsula: The Salines playa lake case study. *Quat. Int.* **2016**, *403*, 187–200. [CrossRef]
104. Pérez Jordà, G.; Alonso Martínez, N.; Iborra Eres, M.P. Agricultura y ganadería protohistóricas en la Península Ibérica: Modelos de gestión. In *Arqueología de la Tierra: Paisajes Rurales de la Protohistoria Peninsular: VI Cursos de Verano Internacionales de la Universidad de Extremadura (Castuera, 5–8 de Julio de 2005)*; Universidad de Extremadura, Servicio de Publicaciones: Cáceres, Spain, 2007; pp. 327–372.
105. Pérez Jordà, G. La Agricultura en el País Valenciano Entre el VI y el I Milenio a.C. Ph.D. Thesis, Universitat de València, Valencia, Spain, 2013; p. 374.
106. Gisbert Santonja, J.A. *El Tossalet de les Mondes (Pego)*; Univ. de València, Saguntum: Valencia, Spain, 1993; pp. 207–231.

107. Aranegui Gascó, C. *El Sucronenesis Sinus en Época Ibérica. Saguntum Extra*; Univ. de València, Saguntum: Valencia, Spain, 2015; p. 201.
108. Barton, C.M. Complexity, social complexity, and modeling. *J. Archaeol. Method Theory* **2014**, *21*, 306–324. [CrossRef]